Smart-Grid Monitoring: Enhanced Machine Learning for Cable Diagnostics

Yinjia Huo, Gautham Prasad, Lutz Lampe, and Victor C. M. Leung
Department of Electrical and Computer Engineering, The University of British Columbia
Email: {yortka, gauthamp, lampe, vleung}@ece.ubc.ca

***Abstract*—Recent works have shown the viability of reusing power line communication modems present in the distribution network for cable diagnostics. By integrating machine learning (ML) techniques, power line modems (PLMs) are shown to be capable of automatically detecting, locating, and assessing different types of cable degradations and faults by monitoring and analyzing their estimated channel frequency responses. However, a single ML algorithm is not ideal for all different diagnostics tasks. To aid us in choosing the most suitable ML algorithm(s) for each of the tasks and to make our solution layman accessible, we propose the use of automated ML, which automatically constructs the best ML model from various algorithms and preprocessing techniques for any given diagnostics task. Our proposed diagnostics approach accelerates the practical deployment of PLM-based grid monitoring by providing a ready-to-use solution to utilities that can be applied without detailed domain knowledge of ML operations.**

***Index Terms*—Smart grid monitoring, cable diagnostics, asset monitoring, machine learning, AutoML**

I. Introduction

Seamless operation of the power grid and a continuous supply of electricity are vital for our daily life. However, reliability of the aging grid infrastructure is reducing as it suffers from considerable underinvestment and increasing congestion levels, and is also subject to inadequate maintenance and upgrades [1, Ch. 2]. This renders several grid assets vulnerable to in-service failures causing power outages and resultant economic losses [2]. Among these assets, in this work, we focus on damages to power cables, where an untreated power cable exposed to extended periods of cable degradations is susceptible to an eventual fault. To avoid such hazardous situations, several cable diagnostics schemes have been developed in the past to identify issues in the cable, such that preventive actions could be taken to avoid a possible cable in-service fault [3, Ch. 6].

Conventional cable diagnostics methods carry several drawbacks. They typically involve high implementation cost by requiring dedicated test equipments and manual data interpretation [4]–[10]. Furthermore, many of these techniques operate only on de-energized cables, and therefore demand at least a portion of the grid to be shut down before testing. To overcome these drawbacks, a new class of diagnostics solutions was proposed, which makes use of existing power line modems (PLMs) for grid diagnostics [11]–[15]. They reuse the PLMs installed in the grid for smart-grid communication purposes to also perform grid diagnostics by monitoring the communication channel inherently estimated within the legacy PLMs to infer the status of the cable health. The solutions in [12]–[15] additionally integrate machine learning (ML) techniques to design a fully-automated independent cable diagnostics solution that can operate on energized cables to provide utilities with the ability to remotely monitor the distribution grid.

The state-of-the-art cable diagnostics solution in [15] proposes an ML framework for self-reliant diagnostics to progressively detect, assess, and locate cable degradations under varying network load and degradation conditions. However, we learn that a single ML algorithm is not appropriate for all diagnostics tasks. For example, [15] shows that support vector machine (SVM) [16] is more suitable for detecting the presence of a localized degradation, while boosting techniques [17] are preferable for degradation severity assessment. Along similar lines, [14] also demonstrates that varying the power line communication (PLC) transmission bandwidth, or monitoring a different type of degradation, demands different features to be extracted from the communication channel estimate for machine training. These issues motivate us to investigate techniques that could be globally applicable in determining the most suitable ML algorithm/s for any given diagnostics task, and also assist us in choosing the appropriate features needed to be extracted from the raw data (say, channel or signal-to-noise ratio estimates) for efficient machine training and operation.

Our second goal of this work is to design a cable diagnostics solution that is layman accessible. Such a method is appealing to utilities or other cable maintenance enterprises, which can apply our solution without also requiring to employ technical personnel who are experienced in cable condition monitoring or ML operation. This increases the practical applicability and accelerates the deployment of a PLM-based grid diagnostics solution.

To achieve the two outlined goals, we propose an automated ML (AutoML) [18] based diagnostics solution. We use our previous works [13]–[15] as the baseline, and integrate AutoML to automatically determine the most suitable data preprocessing techniques, ML algorithm/s, and the associated hyper-parameters that provide the highest performance in terms of a pre-defined cost function within a fixed computational and memory budget for any given ML task. We expand the possible choices of ML algorithms beyond SVM

This work was supported by the Natural Sciences and Engineering Research Council of Canada (NSERC).

978-1-7281-0289-4/19/$31.00 © 2019 IEEE

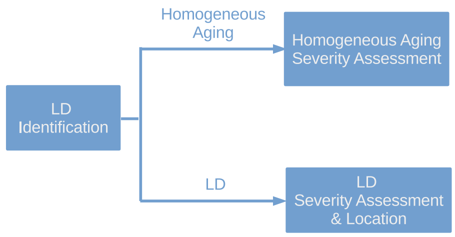

Fig. 1. The ML framework for cable diagnostics [15].

and boosting to include a wider range of algorithms, out of which, we choose one or more to build the most suitable model for any considered diagnostics task. We test our design on a generic medium voltage network topology under varying grid load conditions and evaluate the performance accuracy of our solution. Through these results, we show the significant performance improvement we achieve when compared to the state-of-the-art [15], by obtaining near-ideal accuracy in detecting, locating, and assessing homogeneous and localized cable degradations.

The rest of the paper is organized as follows. We present our ML-based cable diagnostics framework in Section II. In Section III, we detail the procedure to integrate AutoML into our ML framework. We present our simulation results in Section IV and conclude in Section V.

II. Cable Diagnostics

Underground power cables are of either paper-oil or extruded type [19]. Paper-oil cables suffer mainly from thermal degradations, while extruded ones are mostly susceptible to electrical aging, i.e., developing electrical-treeing (ET) and water-treeing (WT) [20]. In this work, we consider the latter type of cables, since extruded cross-linked polyethylene (XLPE) has long been the preferred and widely deployed cable insulation material due to the low processing costs, high reliability, and the suitable electrical and mechanical properties it exhibits [19], [21], [22]. WT degradations are one of the two main causes for premature failures of extruded cables, and also lead to the other main cause, which is ET [3, Ch. 6], [23]. Considering these factors, we focus our investigations on cable aging caused by WT degradations in XLPE cables. Our choice also has the added benefit that the WT growth and the dielectric property of WT-degraded XLPE cables are extensively studied and well-modeled in the literature [24], [10].

WT degradations develop in XLPE cables in either a homogeneous or a localized fashion. Prior observations have shown that a homogeneous near-uniform WT degradation across the cable length is seen under typical operating conditions [24], [25]. However, water ingress, or local defects, such as protruded semiconductor coating and voids, may also lead to a salient localized WT degradation on top of the uniform homogeneous degradation [26]. Therefore, we use a multi-step degradation diagnostics design, shown in Fig. 1, to sequentially diagnose both these types of aging profiles [13], [15].

The first step involves determining the presence of a salient localized degradation (LD). If no LDs are identified, we classify the cable to have undergone homogeneous degradation. We then estimate the degradation severity to determine the extent of WT damage. A healthy cable is subsumed within this condition, where the severity assessment returns near-zero degradation. Note that severity estimation is a crucial component in the broad scheme of diagnostics. One of the goals of cable diagnostics is to achieve fault prediction/anticipation, so that preventive actions can be taken to avoid an in-service failure. Therefore, it is critical to not only identify the presence of a degradation, but also estimate its severity.

When the first step instead indicates the presence of an LD, we proceed to the second step, similar to the earlier case, to determine the degradation severity. However, in LD diagnostics, we additionally estimate the LD location, so that concentrated efforts can be undertaken on the cable. We again note that this is a critical step that ensures a speedy and convenient cable treatment, and addresses one of the major concerns in transitioning power lines into underground cables despite their known benefits [27].

For all the above diagnostics tasks, namely, degradation detection, assessment, and location, we use supervised ML techniques to achieve an automated and independent operation. We train a machine beforehand for every task using the communication channel frequency response (CFR) estimated by the PLM as the raw data from which we extract features[1]. Additionally, along with the traditional end-to-end communication channel, we have shown in our prior works that the reflection channel observed at the modem-line interface can also be used as raw data to obtain greater insight into the cable health [15]. Therefore, we consider both these channel estimates for our diagnostic tasks.

We train separate machines for each of the tasks shown in Fig. 1. We formulate the LD identification as an ML classification problem, while the rest of them as regression problems. In the following sections, we present enhanced ML techniques to automatically select the most suitable ML algorithm/s and their associated hyper-parameters for any given diagnostics task.

III. AutoML for Cable Diagnostics

In our previous work [13], [15], we considered two sets of ML algorithms, SVM [16] and boosting techniques [17]. While we have shown that satisfactory results are achievable for the tasks considered, we expand our algorithm choice set to determine if one or more algorithms can provide more accurate results. In particular, we apply AutoML for automatically selecting the most suitable algorithms, and also for determining the appropriate data/feature preprocessing techniques and hyper-parameters associated with the chosen ML algorithms to optimize the user-defined cost function within a fixed computational and memory budget [18].

[1]The procedure for generating PLC channels of WT degraded XLPE cables using a bottom-up PLC channel emulator along with a WT degradation model can be found in [13].

For our supervised ML operation, we train our machine using CFRs collected in a training set, $\mathcal{D}_{\text{train}}$, along with the labels, y_{train}, corresponding to each entry in $\mathcal{D}_{\text{train}}$. For LD identification, y_{train} contains binary indications of the presence or absence of an LD in the considered CFR. Similarly, for regression tasks, such as degradation severity prediction, y_{train} indicates the degradation severity values associated with the CFRs in $\mathcal{D}_{\text{train}}$. Further, we also use $\mathcal{A}$, Λ, and $\mathcal{P}$ as the set of candidate ML algorithms, their corresponding hyper-parameters, and possible data/feature preprocessing techniques, respectively. We formulate the problem of selecting the most suitable combination of ML algorithms, $a^\star \in \mathcal{A}$, its associated hyper-parameters, $\lambda^\star \in \Lambda$, and the data/feature preprocessing technique $p^\star \in \mathcal{P}$ in practice as

$$(p^\star, a^\star, \lambda^\star) = \underset{p\in\mathcal{P}, a\in\mathcal{A}, \lambda\in\Lambda}{\operatorname{argmin}} \; \mathcal{L}(a(p(\mathcal{D}_{\text{train}}), \lambda), y_{\text{train}}), \tag{1}$$

where $\mathcal{L}$ is the pre-defined cost function[2], e.g., cross entropy for classification, or mean squared error (MSE) for regression.

For our software implementation of AutoML, we use the Auto-SKLearn [18]. Auto-SKLearn builds on the existing AutoML methods in the literature by using meta-learning and automatic ensemble construction techniques to provide increased efficiency and robustness. The meta-learning approach is used to initialize the Bayesian optimizer of the random-forest-based sequential model-based algorithm configuration [28], which is used to fine tune the performance of hyper-parameter space instantiations. Further, the automatic ensemble construction ensures that we are less prone to over-fitting and results in improved performance, especially when instantiations for constructing the ensemble causes uncorrelated prediction error. Thereby, Auto-SKLearn improves over state-of-the-art AutoML in terms of both implementation and performance. A detailed description of Auto-SKLearn can be found in [18].

IV. Results

In this section, we evaluate the performance of our ML framework of Fig. 1 using Auto-SKLearn. For our evaluations, we use a computation time limit for the AutoML of one hour on a laptop computer with no storage use limit. However, note that off-line training performed at, say, the central office of utilities, is equipped with much larger computational capacity, and we could, therefore, expect to obtain results with greater accuracy in practice. We use both the traditional end-to-end PLC CFR estimated by PLMs, H_{e2e}, as well as the reflection channel, H_{ref}, as raw data for feature extraction. We denote the total number of training and testing samples used for every task as n_{TR} and n_{TE}, respectively.

A. Network Topology

We apply a T-network that can be used as a building block to construct any complicated network topology. However, typical medium-voltage networks, which are commonly radial in nature, consist of few branches with segment lengths that are beyond the coverage of a single PLM [29]. Therefore, a T-network with PLMs at each node-ends well-represents a practical topology. Specifically, we consider a network as shown in Fig. 2, with equal segment lengths of all cables. Additionally, we also capture possible extensions beyond each of the PLMs that could lead to the issue of topological ambiguity while detecting or locating a localized defect [11], [30]. E.g., when PLM-$i, i \in \{1, 2, 3\}$ determines the presence of a defect, it is unable to ascertain if the defect lies in the considered network (CN) or on a branch in the neighboring network. To address this challenge, we apply a cooperative diagnostics approach shown in Fig. 3.

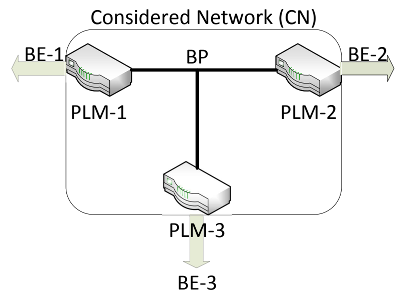

Fig. 2. Portion of the distribution network considered with possible branch extensions (BEs) beyond each PLM.

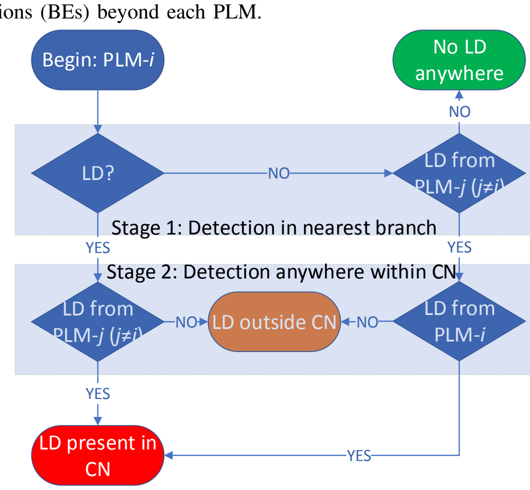

Fig. 3. The cooperative diagnostics approach we employ at every PLM, with $i, j \in \{1, 2, 3\}$, to resolve topological ambiguity during LD identification, where PLMs look for an LD in the nearest branch in Stage 1, and, in Stage 2, cooperatively confirm the presence of an LD in CN by looking for an LD anywhere within the CN.

When the first stage of our diagnostics task, i.e., LD identification, indicates a homogeneous aging profile in the cable, we use the WT growth model of [24] to calculate an equivalent age, t_{eq}, as an indication of overall aging condition along the cable sections. On the other hand, if an LD present in the considered network, we conduct both the LD severity assessment as well as degradation location. The LD severity, γ_{local}, is defined as the portion of the WT degraded cable insulation in a cable cross-section as compared to the total insulation thickness (see [13, Fig. 1]). To ensure that a salient LD is distinct against homogeneous aging, we confine

[2] Note that the target of any ML task is to minimize the cost function evaluated for future test samples, i.e., $\min \mathcal{L}(a(p(\mathcal{D}_{\text{test}}), \lambda), y_{\text{test}})$. However, since $\mathcal{D}_{\text{test}}$ is inaccessible in practice during the training phase, we use $\mathcal{D}_{\text{train}}$, which is generated synthetically, and whose samples are identically distributed with $\mathcal{D}_{\text{test}}$.

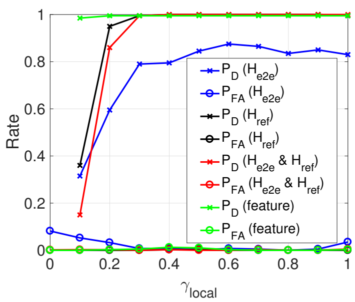

Fig. 4. Detection rates (P_{D}) and false alarm rates (P_{FA}) obtained in identifying the presence of an LD in the nearest branch to the PLM.

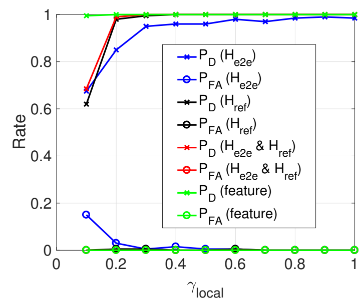

Fig. 5. Detection rates (P_{D}) and false alarm rates (P_{FA}) obtained in determining the right branch on which the LD lies.

TABLE I

RMSE Performance of Regression Tasks*

Training Data	t_{eq} Sec. IV-B2	γ_{local} Sec. IV-B3	Target Sec. IV-B4	$\gamma_{\mathsf{local}}\ell_{\mathsf{WT}}$ Sec. IV-B4
H_{e2e}	**0.1212**	0.0412	28.16	5.98
H_{ref}	0.6196	0.0648	23.1	9.51
H_{e2e} & H_{ref}	0.0.1817	0.05	25.77	6.6
Feature	0.7769	**0.0134**	**0.6618**	**3.41**
RMSE in [15]	1.4724	0.0253	3.0583	6.76

*We omit the units for brevity.

$0.1 \leq \gamma_{\mathsf{local}} \leq 1$. We perform the LD location in two parallel steps; predicting the *target* location, i.e., the distance from the PLM to the near end of the LD, and estimating of its length, ℓ_{WT}.

B. Numerical Results

1) LD Identification: We use $n_{\mathsf{TR}} = 7000$ for LD identification. Among these, we set 1000 with a homogeneous aging profile containing no salient localized WT degradation. We then introduce LD on one of the six branches of Fig. 2 for the next 1000 samples, and perform the same for all the remaining five branches. We use a cooperative diagnostics approach specified in Fig. 3 to detect a possible LD between any PLM-i and BP. We feed in the 7000 known samples in $\mathcal{D}_{\mathsf{train}}$ and the corresponding $y_{\mathsf{train}} \in \{\text{"positive"}, \text{"negative"}\}$ to Auto-SKLearn.

The results of the two stages of LD identification are shown in Fig. 4 and Fig. 5, respectively, for varying γ_{local}. We illustrate the results that we obtain by using different raw data in $\mathcal{D}_{\mathsf{train}}$. Detection rates obtained using H_{e2e} as raw data show unsatisfactory results across all γ_{local}. However, the rates are substantially improved by using H_{ref}, either independently or in conjunction with H_{e2e}. For comparison, we also show an additional result that we obtain by extracting features from H_{e2e} and H_{ref} manually before feeding the values into Auto-SKLearn. We detail the feature extraction procedure in the Appendix. We observe that this provides near-ideal detection and false alarm rates, which are only matched by feeding raw data to AutoML beyond $\gamma_{\mathsf{local}} \geq 0.3$. This shows that while using raw data directly simplifies implementation procedures without incurring the effort of feature extraction, its performance suffers in detecting LDs of low degradation severity.

2) Homogeneous Aging Assessment: When LD identification indicates the absence of an LD, we classify the cable

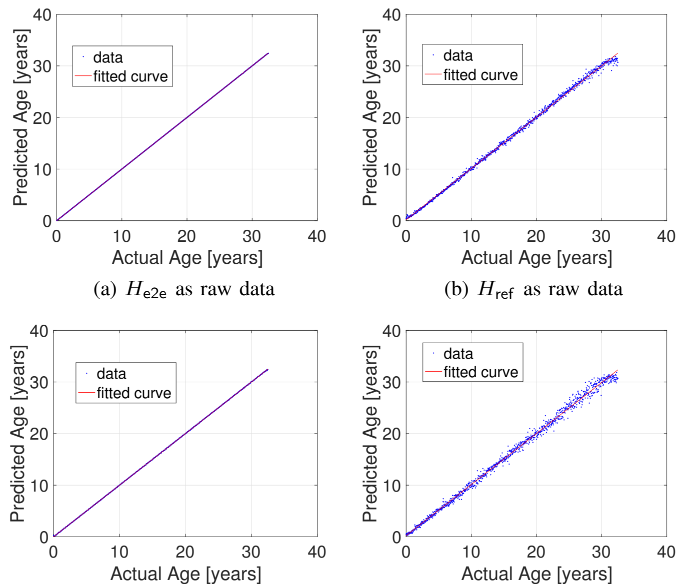

(a) H_{e2e} as raw data (b) H_{ref} as raw data (c) H_{e2e} and H_{ref} as raw data (d) Manually extracted features

Fig. 6. Prediction accuracy in estimating the equivalent cable age that has undergone homogeneous WT degradation, with $(n_{\mathsf{TR}}, n_{\mathsf{TE}}) = (3600, 1000)$.

to be subject to homogeneous degradation. To estimate the extent of degradation, we feed the known CFRs in $\mathcal{D}_{\mathsf{train}}$ with their associated equivalent ages as labels in y_{train}, into the Auto-SKLearn tool. We show the performance of our severity estimation in Fig. 6. We ideally expect all our predictions to match the actual equivalent age of the cable, i.e., the fitted curve to be a unit-slope line passing through the origin. We notice in Fig. 6(a)-(d) that we nearly obtain such a condition under all considered scenarios, which are, using H_{e2e} and/or H_{ref} as raw data, and applying manual feature extraction. However, we observe that individual predictions vary in each of these cases, as quantified by the root mean squared error (RMSE) in Table I. We note that for the task of predicting the equivalent age, t_{eq}, using H_{e2e} independently as the raw data provides the least RMSE. This also shows the superiority of AutoML in automatically extracting favorable features from the raw data for this prediction task.

3) LD Severity Assessment: When our first task of LD identification indicates the present of an LD, we begin by estimating its degradation severity. Similar to the process in Section IV-B2, we input known CFRs in $\mathcal{D}_{\mathsf{train}}$ and their asso-

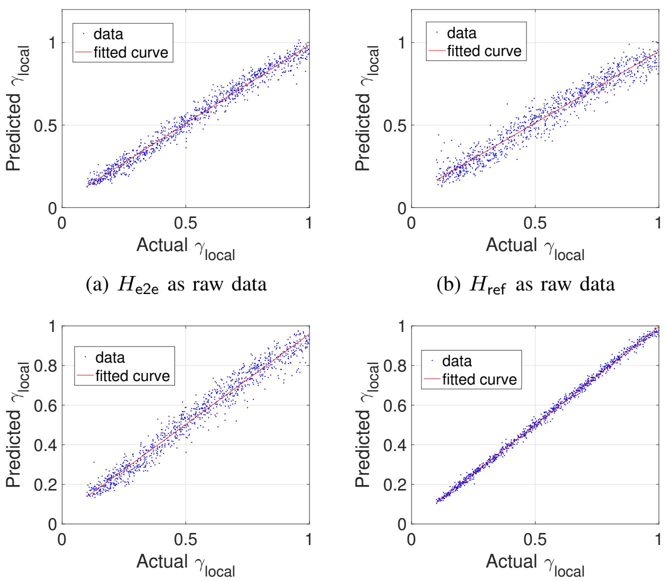

(a) H_{e2e} as raw data (b) H_{ref} as raw data (c) H_{e2e} and H_{ref} as raw data (d) Manually extracted features

Fig. 7. Prediction accuracy in assessing the LD severity, with $(n_{\text{TR}}, n_{\text{TE}}) = (3600, 1000)$.

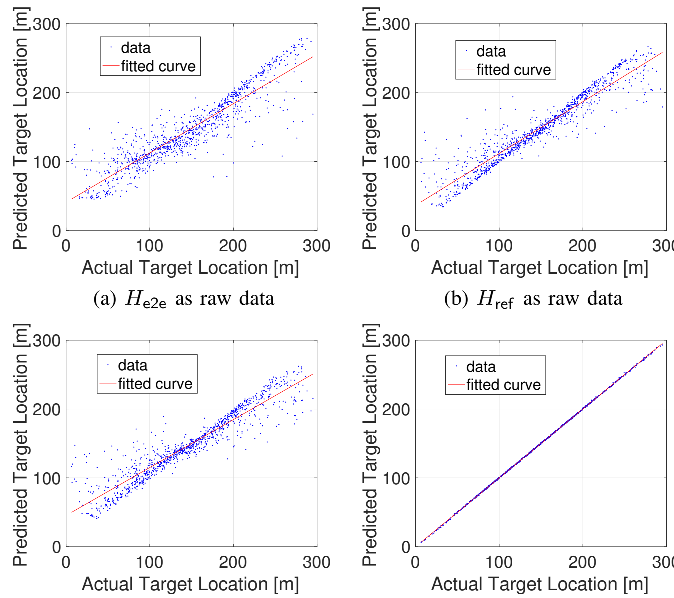

(a) H_{e2e} as raw data (b) H_{ref} as raw data (c) H_{e2e} and H_{ref} as raw data (d) Manually extracted features

Fig. 8. Prediction accuracy in locating the near-end of the LD (target), with $(n_{\text{TR}}, n_{\text{TE}}) = (3600, 1000)$.

ciated γ_{local} in y_{train}, into Auto-SKLearn to train a regressor. The performance results obtained while testing this machine are shown in Fig. 7. From the fitted curve in Fig. 7 and RMSE values in Table I, we observe that the prediction performance is most accurate when we extract features from the raw data manually, instead of relying on AutoML for the feature extraction. Nevertheless, the chosen set of ML algorithms by AutoML enables us to achieve superior prediction results when compared to the state-of-the-art in [15, Fig. 10(b)], by reducing the RMSE of the predictions by over 47%.

4) LD Localization: Our final diagnostics task is to precisely locate the position of the detected LD, i.e., to predict the locations of its two ends. To this end, we rely on the PLM that is closest to the LD for this task. We first locate the distance of the near-end of the LD to the PLM, which we refer to as the *target* location. The training procedure for target location follows similar ones employed in Section IV-B2 and Section IV-B3. The performance of such a trained machine is shown in Fig. 8 and Table I. We notice that automatic feature extraction from ML does not provide satisfactory prediction accuracy, whereas extracting features manually provides significant improvement in the estimation precision, as well as a multi-fold reduction in the RMSE. Further, AutoML continues to outperform results in [15, Fig. 11(a)] in terms of RMSE, due to its superior approach of automatically constructing the optimized ensemble from a wider range of available ML algorithms and the employed data/feature preprocessing methods.

To predict the far-end of the LD, we estimate its degradation length, ℓ_{WT}. However, we achieve unsatisfactory results when we attempt to directly estimate ℓ_{WT}. As a work-around, we instead estimate the product, $\gamma_{\text{local}} \cdot \ell_{\text{WT}}$, and then use the predicted values of γ_{local} from Section IV-B3 to obtain an estimate for ℓ_{WT}. The results of this exercise using AutoML is shown in Fig. 9 and Table I, where we notice that although all results provide near-ideal fitted prediction curve, extracting features manually provides lower RMSE.

C. Outlook

Based on the results in Fig. 4-9, we observe the following. The use of AutoML for automatically constructing the optimized ensemble of ML algorithms along with automated data and feature preprocessing techniques provide superior results over the state-of-the-art in [15] for all diagnostics tasks we outlined in Fig. 1. Further, using H_{ref} in place of H_{e2e} increases the rate of detecting LDs. However, H_{e2e} provides greater insight into homogeneous WT degradations over H_{ref}. Therefore, it is suitable to use both these CFRs in conjunction with each other. Finally, if we can manually extract feature from the raw data, Auto ML can be used to significantly improve performance compared to conventional ML approaches. However, a fully automated training procedure using AutoML provides a layman accessible solution that can also provide enhanced results over state-of-the-art ML designs without requiring a detailed domain knowledge of the considered task.

V. Conclusion

In this paper, we have presented an automated machine learning based cable diagnostics design. Our solution automatically determines the most suitable data preprocessing techniques, machine learning algorithms, and the associated hyper-parameters required to obtain the optimal performance in terms of a user-defined cost function for any given diagnostics task within a fixed computational and memory budget. For software implementation purposes, we used the Auto-SKLearn toolkit, which enhances existing AutoML methods by using meta-learning and automatic ensemble construction to provide

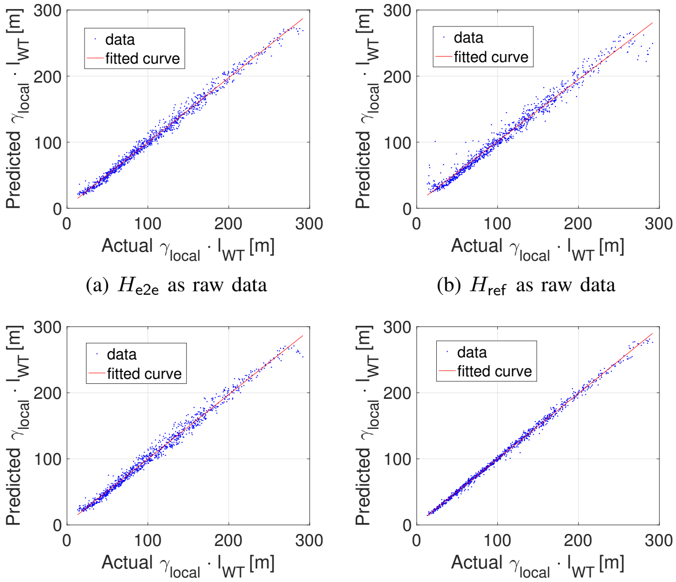

(a) H_{e2e} as raw data (b) H_{ref} as raw data

(c) H_{e2e} and H_{ref} as raw data (d) Manually extracted features

Fig. 9. Prediction accuracy of $\gamma_{\mathrm{local}} \cdot \ell_{\mathrm{WT}}$, with $(n_{\mathrm{TR}}, n_{\mathrm{TE}}) = (3600, 1000)$.

increased efficiency and robustness. Through simulation results, we devised strategies to suitably adapt Auto-SKLearn for various cable diagnostics tasks that enable us to obtain near-ideal performance accuracy. Our solution is layman accessible, and can be used without detailed knowledge about machine learning algorithms or cable degradation characteristics.

APPENDIX

In this appendix, we detail the set of features that we include in our library for manual feature extraction. As discussed in detail in [13]–[15], cable degradations cause higher dielectric losses [25] and slower wave propagation speeds [31]. To capture these two effects, we include mth-order moments ($m \in \{1, 2, 3, 4\}$) of the magnitude and phase of H_{e2e} and H_{ref} in our manually extracted features. Further, LDs cause discontinuities in the dielectric properties along the cable insulation. Therefore, we also include the peak locations and their magnitudes observed in the time-domain versions of H_{e2e} and H_{ref} in our feature library. However, note that we manually select only those set of features that are most suitable for the considered diagnostics task.

REFERENCES

[1] S. Fawkes, *Energy efficiency: the definitive guide to the cheapest, cleanest, fastest source of energy*. Routledge, 2016.
[2] F. J. Shields, "The problem of arcing faults in low-voltage power distribution systems," *IEEE Trans. Ind. Appl.*, vol. IGA-3, no. 1, pp. 15–25, 1967.
[3] P. Gill, *Electrical power equipment maintenance and testing*. CRC press, 2008.
[4] P. Wang, M. R. Raghuveer, W. McDermid, and J. C. Bromley, "A digital technique for the on-line measurement of dissipation factor and capacitance," *IEEE Trans. Dielectr. Electr. Insul.*, vol. 8, no. 2, pp. 228–232, 2001.
[5] V. Dubickas, "On-line time domain reflectometry diagnostics of medium voltage xlpe power cables," Ph.D. dissertation, KTH, 2006.
[6] L. A. Griffiths, R. Parakh, C. Furse, and B. Baker, "The invisible fray: A critical analysis of the use of reflectometry for fray location," *IEEE Sensors J.*, vol. 6, no. 3, pp. 697–706, 2006.
[7] A. Cozza and L. Pichon, "Echo response of faults in transmission lines: Models and limitations to fault detection," *IEEE Trans. Microw. Theory Tech.*, vol. 64, no. 12, pp. 4155–4164, 2016.
[8] A. Manet, A. Kameni, F. Loete, J. Genoulaz, L. Pichon, and O. Picon, "Equivalent circuit model of soft shield defects in coaxial cables using numerical modeling," *IEEE Trans. Electromagn. Compat.*, vol. 59, no. 2, pp. 533–536, 2017.
[9] R. Liao, J. Hao, G. Chen, and L. Yang, "Quantitative analysis of ageing condition of oil-paper insulation by frequency domain spectroscopy," *IEEE Trans. Dielectr. Electr. Insul.*, vol. 19, no. 3, 2012.
[10] G. Mugala, "High frequency characteristics of medium voltage xlpe power cables," Ph.D. dissertation, KTH, 2005.
[11] A. M. Lehmann, K. Raab, F. Gruber, E. Fischer, R. Müller, and J. B. Huber, "A diagnostic method for power line networks by channel estimation of PLC devices," in *IEEE Int. Conf. on Smart Grid Commun. (SmartGridComm)*, 2016, pp. 320–325.
[12] L. Förstel and L. Lampe, "Grid diagnostics: Monitoring cable aging using power line transmission," in *IEEE Int. Symp. Power Line Commun. Appl. (ISPLC)*, 2017, pp. 1–6.
[13] Y. Huo, G. Prasad, L. Atanackovic, L. Lampe, and V. C. M. Leung, "Grid surveillance and diagnostics using power line communications," in *IEEE Int. Symp. Power Line Commun. Appl. (ISPLC)*, 2018, pp. 1–6.
[14] Y. Huo, G. Prasad, L. Lampe, and V. C. M. Leung, "Cable health monitoring in distribution networks using power line communications," in *IEEE Int. Conf. Commun. Control Computing Tech. Smart Grids (SmartGridComm)*, 2018, pp. 1–6.
[15] Y. Huo, G. Prasad, L. Atanackovic, L. Lampe, and V. C. M. Leung, "Cable diagnostics with power line modems for smart grid monitoring," *arXiv preprint arXiv:1808.01149*, 2018.
[16] M. A. Hearst, S. T. Dumais, E. Osuna, J. Platt, and B. Scholkopf, "Support vector machines," *IEEE Intell. Syst. Applicat.*, vol. 13, no. 4, pp. 18–28, 1998.
[17] R. E. Schapire, "The boosting approach to machine learning: An overview," in *Nonlinear estimation and classification*. Springer, 2003, pp. 149–171.
[18] M. Feurer, A. Klein, K. Eggensperger, J. Springenberg, M. Blum, and F. Hutter, "Efficient and robust automated machine learning," in *Advances Neural Inform. Proc. Syst. 28*. Curran Associates, Inc., 2015, pp. 2962–2970.
[19] H. Orton, "History of underground power cables," *IEEE Electr. Insul. Mag.*, vol. 29, no. 4, pp. 52–57, 2013.
[20] J. Densley, "Ageing mechanisms and diagnostics for power cables - an overview," *IEEE Electr. Insul. Mag.*, vol. 17, no. 1, pp. 14–22, 2001.
[21] P. Fairley, "Utilities bury more transmission lines to prevent storm damage," *IEEE Spectrum*, vol. 2, pp. 9–10.
[22] T. L. Hanley, R. P. Burford, R. J. Fleming, and K. W. Barber, "A general review of polymeric insulation for use in hvdc cables," *IEEE Electr. Insul. Mag.*, vol. 19, no. 1, pp. 13–24, 2003.
[23] R. Patsch and J. Jung, "Water trees in cables: Generation and detection," *IEE Proc. Sc. Meas. Technol.*, vol. 146, no. 5, pp. 253–259, 1999.
[24] J. P. Crine and J. Jow, "A water treeing model," *IEEE Trans. Dielectr. Electr. Insul.*, vol. 12, no. 4, pp. 801–808, 2005.
[25] P. Werelius, "Development and application of high voltage dielectric spectroscopy for diagnosis of medium voltage XLPE cables," Ph.D. dissertation, KTH, 2001.
[26] J. P. Crine, "Electrical, chemical and mechanical processes in water treeing," *IEEE Trans. Dielectr. Electr. Insul.*, vol. 5, no. 5, pp. 681–694, 1998.
[27] Head to head - overhead vs underground. [Online]. Available: https://westernpower.com.au/community/news-opinion/head-to-head-overhead-vs-underground/
[28] F. Hutter, H. H. Hoos, and K. Leyton-Brown, "Sequential model-based optimization for general algorithm configuration," in *Intl. Conf. Learning Intell. Optimization*. Springer, 2011, pp. 507–523.
[29] S. Abeysinghe, J. Wu, M. Sooriyabandara, M. Abeysekera, T. Xu, and C. Wang, "Topological properties of medium voltage electricity distribution networks," *Appl. Energy*, vol. 210, pp. 1101–1112, 2018.
[30] A. Bahmanyar, S. Jamali, A. Estebsari, and E. Bompard, "A comparison framework for distribution system outage and fault location methods," *Electr. Power Syst. Research*, vol. 145, pp. 19–34, 2017.
[31] H. Livani and C. Y. Evrenosoglu, "A machine learning and wavelet-based fault location method for hybrid transmission lines," *IEEE Trans. Smart Grid*, vol. 5, no. 1, pp. 51–59, 2014.